Effect of Temperature on In-Use Stiction of Cantilever Beams Coated With Perfluorinated Alkysiloxane Monolayers

Joëlle Fréchette, Roya Maboudian, and Carlo Carraro

***Abstract*—The effect of annealing (for temperatures up to 300 °C) on the antistiction performance of perfluorinated self-assembled monolayers (SAMs) is characterized using polycrystalline Si cantilever beam arrays. The monolayers 1H,1H,2H,2H, perfluorodecyltrichlorosilane (FDTS) and 1H,1H,2H,2H, perfluorodecyldimethylchlorosilane (FDDMCS) deposited from both liquid and vapor phase are investigated. It is observed that stiction *decreases* upon annealing for both monolayers and for both types of deposition. FDTS, however, displays greater temperature stability than FDDMCS regardless of the mode of deposition. The higher thermal resistance of the FDTS underscores the importance of monolayer crosslinking since unlike FDDMCS, FDTS forms a siloxane network on the surface. Further vacuum annealing and X-ray photoelectron spectroscopy experiments are performed to identify chemical changes in the monolayer during annealing. Incipient monolayer degradation is observed, with loss of the whole fluorinated monolayer chain. This process appears drastically different from the decomposition mechanism of hydrogenated alkylsiloxane monolayers such as octadecyltrichlorosilane (OTS). [1637]**

***Index Terms*—Microelectromechanical systems (MEMS), monolayer coating, stiction, thermal stability.**

I. Introduction

MICROELECTROMECHANICAL systems (MEMS) produced by surface micromachining are complex structures consisting of layers of thin films (most commonly, polycrystalline silicon or polysilicon). Due to their large aspect ratios and their microscale dimensions, these devices are highly susceptible to interfacial forces. These interfacial forces often cause unwanted interactions (friction, adhesion, and wear) that can be a major reliability concern for the MEMS industry [1]–[4]. In recent years, significant progress has been made towards the development and implementation of surface coatings designed to reduce the unwanted adhesion (also called stiction) in MEMS [1], [5]. This effort has resulted in devices with very low adhesion and in a better understanding of how different surface treatments affect the interfacial behavior of a microdevice.

Manuscript received June 25, 2005; revised January 12, 2006. This work was supported by the National Science Foundation (under Grant DMI-0355339) and UC Discovery/Robert Bosch Corporation. Subject Editor C. Liu.

J. Fréchette was with the Department of Chemical Engineering and Berkeley Sensor and Actuator Center, University of California, Berkeley, CA 94720 USA. She is now with the Department of Chemical and Biomolecular Engineering, Johns Hopkins University, Baltimore, MD 21218 USA.

R. Maboudian and C. Carraro are with the Department of Chemical Engineering and Berkeley Sensor and Actuator Center, University of California, Berkeley, CA 94720 USA (e-mail: carraro@berkeley.edu).

Digital Object Identifier 10.1109/JMEMS.2006.878893

However, with very few exceptions [6]–[8], the impact of surface treatments on adhesion has only been investigated for the usual conditions of room temperature, and in air under low to moderate relative humidity. While the impact of temperature on the integrity of some self-assembled monolayer (SAM) typically deposited on Si(100) surfaces has been somewhat investigated [9]–[13], there is a need to understand how well SAM coatings can maintain their antistiction properties when exposed to elevated temperatures. This is especially important considering the likelihood a micromachine is exposed, during packaging or its use, to higher temperatures or otherwise different conditions than ambient. Moreover, studying adhesive behavior at high temperature may prove useful in developing accelerated testing protocols for in-use stiction.

Fluorinated monolayers are promising antistiction coatings for MEMS devices because they are highly hydrophobic and oleophobic [14]. In addition, perfluoroalkylsiloxane monolayers have been shown to maintain their hydrophobicity even after being exposed to temperatures up to 300 °C [15]. In this work, we have investigated the thermal stability of two fluorinated alkylsiloxane monolayers, derived from the precursor molecules 1H,1H,2H,2H, perfluorodecyltrichlorosilane ($CF_3(CF_2)_7(CH_2)_2SiCl_3$, DTS) and 1H,1H,2H,2H, perfluorodecyldimethylchlorosilane ($CF_3(CF_2)_7(CH_2)_2(CH_3)_2SiCl$, FDDMCS). These two monolayers are almost identical, except that the precursor molecules have different end groups. FDTS has three chlorosilane bonds creating likely a crosslinked monolayer on the silicon surface. In contrast, FDDMCS has only one chlorosilane group and therefore it does not form a siloxane network on the surface. The effect of FDTS on reducing stiction is well documented [8], [16], [17]. FDDMCS, on the other hand, has been studied to a lesser extent [18]. In addition, very little is known about the structure of these perfluorinated monolayers when exposed to elevated temperatures. Fluorinated monolayers adsorbed on aluminum have shown to reversibly rearrange at temperatures as low as 150°C [19] and irreversibly at higher temperatures. It is, therefore, of paramount importance to assess if exposure of a device to high temperature destabilizes the monolayer and causes an increase in stiction.

In this paper, the effect of thermal annealing in air for fluorinated monolayers deposited both from the liquid phase and the vapor phase is presented. Vapor phase monolayer deposition has the advantage of generating substantially fewer particulate residues on the surfaces than liquid deposition [16], [20]. This reduction in the amount and size of agglomerates on the surface is suggested as the reason why vapor deposited monolayers are less prone to stiction than those deposited from the liquid

phase. Regardless of deposition method, our results demonstrate that monolayer head-group functionality is the main factor determining their thermal stability: the trifunctional FDTS monolayer is much more stable than the monofunctional FDDMCS monolayer.

II. Experimental

A. Materials

Monolayer precursors FDTS (96%) and FDDMCS (90%) are obtained from Lancaster Synthesis and are used without further purification. All solvents are reagent grade (isopropyl alcohol, isooctane) and used without purification. De-ionized water is obtained from a Nanopure system (18 $\mathrm{M}\Omega$). All reagents used in vapor coatings have undergone several freeze-pump-thaw cycles before use.

B. Coating Process

The release protocol for the micromachines has been described elsewhere [21], but is summarized here for completeness. The sacrificial oxide on all dice is first etched in HF:HCl (1:1) for 90 min followed by a water rinse; the dice are then cleaned in piranha solution for 15 min. Samples to be coated in liquid phase follow a series of miscible rinses (water, isopropyl alcohol, isooctane) and are then put in a ca. 1 mM monolayer precursor solution (in isooctane) until no change in static contact angle is observed (1 h for LFDTS, 8 h for LFDDMCS). The chips are then successively rinsed back to a water solution and dried in air for 24 h before adhesion is measured.

Samples to be coated from vapor phase are transferred to a methanol solution and dried using CO_2 critical point drying to reveal an oxide surface. The released chips are then placed in a low-pressure reactor [16] where oxygen plasma is applied (3–4 min, 300 mtorr, 50 W), followed by water plasma (3–4 min, 300 mtorr, 50 W). A vial containing FDTS is then heated using boiling water and the vapor is introduced in the reactor (to reach 450 mtorr). Water vapor is then dosed to reach a total pressure of 1.2 torr. After 20 min, the system is pumped down and this operation is repeated to ensure a good quality coating on the surface. The process for depositing FDDMCS from vapor (V-FDDMCS) is similar to the V-FDTS but more cycles are required to reach a good coverage (usually around 5–8 cycles). Static contact angle is measured after each cycle on a Si(100) test chip to monitor the progression in the monolayer coverage.

C. Characterization Methods

Adhesion is measured using the cantilever beam array method (CBA) described elsewhere [22]. The test structures used in this study were fabricated in the Sandia SUMMiT $\mathrm{IV}^{\mathrm{tm}}$ process. Each investigated die contains three cantilever beam arrays (CBA). Each array has 32 beams with lengths varying between 150 and 1700 $\mu\mathrm{m}$ with 50 $\mu\mathrm{m}$ increments. Room temperature actuation is done under normal laboratory ambient conditions, 20 °C and 40% relative humidity. Actuation at various annealing temperatures is accomplished by using a probe station equipped with a heating stage. The stage is heated to the desired temperature, calibrated using a thermocouple at the surface of a Si(100) test chip. Once the desired temperature is reached, the micromachines are placed on the stage and adhesion is measured. The micromachines are exposed to each annealing temperature for 15 min, after which they are removed from the heated stage and cooled down to room temperature. After each annealing (100, 200, 300 °C) the cantilever beam arrays are actuated at room temperature. After each adhesion measurement (at room temperature and at all annealing temperatures) the cantilever beams are mechanically removed from contact to allow for subsequent actuation. A Si(100) piece is subjected to the same treatments (from the piranha etch, to coating, to annealing) and is used to image the monolayers with AFM and to measure contact angle. The annealing pattern used in most of the work described here is shown in Fig. 1. Actuation is done by applying a 110 V dc square wave for 10 cycles. The probing system used for all micromachine actuations is a Lucas-Signatone S-1160 with a Mitutoyo FineScope 60 microscope, equipped with a Sony CCD-IRIS camera. The detachment length (l_{d}) is determined from sticking probability $(P(l_{\mathrm{i}}))$ and is obtained from

$$l_d \approx l_c + \sum_{i=l_{\min}}^{i=l_{\max}} \left[1 - P(l_i)\right] \Delta l$$
$$l_c = l_{\min} - \Delta l \tag{1}$$

where Δl is the beam length increment (50 $\mu\mathrm{m}$ in this case), $l_{\min}$ and $l_{\max}$ are the length of the shortest (150 $\mu\mathrm{m}$) and longest (1700 $\mu\mathrm{m}$) beams, and l_c is a correction for the absence of beams with lengths shorter than $l_{\min}$ [21]. The apparent work of adhesion (W) can be extracted from the detachment length from [22]

$$W = \frac{3Eh^2t^3}{8l_d^4} \tag{2}$$

where E is the Young modulus of polysilicon (170 GPa), h is the height of the beam above the substrate (2 $\mu\mathrm{m}$), and t is the beam thickness (2.5 $\mu\mathrm{m}$). Differential interference contrast interferometry (DIC) and Mirau interferometry are used to determine which beams remain adhered to the landing pad after actuation.

A Digital Instruments Nanoscope III atomic force microscope is used in tapping mode to image the surfaces and quantify their roughness. AFM is used to image the Si(100) surfaces as well as the micromachines (landing pads and under the beams) before and after annealing. Imaging the micromachines with AFM is destructive, thus, cantilever beams and landing pads imaged at room temperature are never actuated at higher temperatures. Static contact angle measurements are performed with a Ramé–Hart 100 A goniometer using DI water (18 $\mathrm{M}\Omega$) and spectroscopic grade hexadecane.

X-ray photoelectron spectroscopy (XPS) is used to characterize the chemical composition and bonding configuration of the monolayer coatings. Photoelectron spectra are acquired in an ultrahigh vacuum (UHV) chamber (base pressure 10^{-9} torr) using a hemispherical analyzer (Omicron EA125) and a nonmonochromated Mg-Kα excitation source (DAR400) at a 70° angle from the detector. The take-off angle is kept fixed along the surface normal in all experiments. Since all recorded spectra are obtained from monolayers deposited on single crystalline Si(100) wafers, binding energies are conveniently referred to the elemental Si2p line fixed at 99.3 eV. Spectra obtained in wide scans show sharp lines corresponding to F1s, O1s, C1s, Si2s, and Si2p photoelectrons, as well as F, O, and C Auger lines. High resolution spectra are obtained in the F1s, O1s, C1s, and Si2p regions, and deconvoluted into series of single peaks (assumed to be pure Gaussians with FWHM of

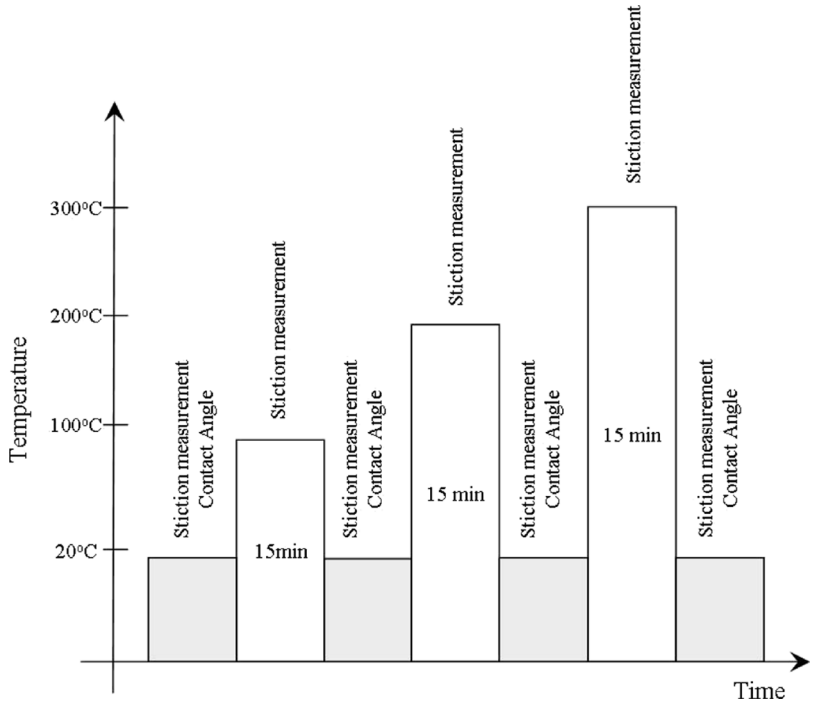

Fig. 1. Annealing pattern used for the measurement of adhesion. The micromachine and Si(100) test chips are annealed at each temperatures for 15 min.

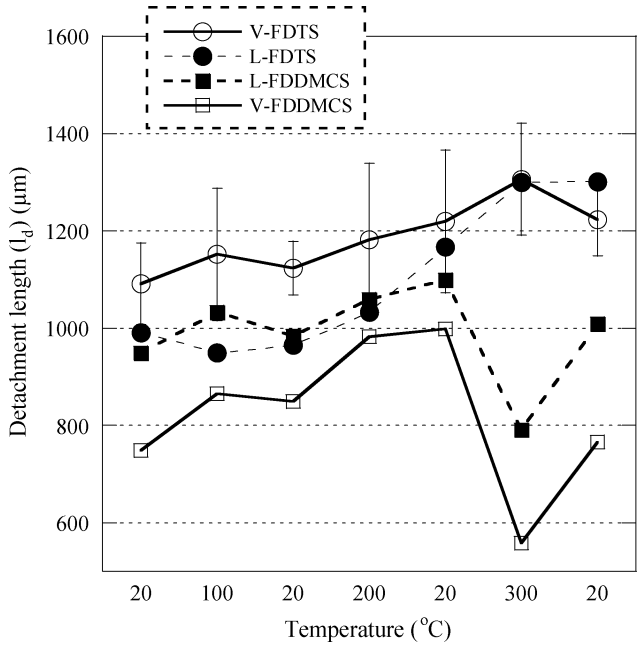

Fig. 2. Temperature dependence of the detachment length (l_d) for all the monolayers investigated. Note that the detachment length is a measure of the sticking probability and is inversely related to the apparent work of adhesion. The error bar for the V-FDTS sample corresponds to the standard deviation for four separate chips, each released and coated separately.

1.7 eV), after Shirley background subtraction. Peak areas are then used to compute elemental ratios [23] after correcting for analyzer transmission [24], photoionization cross sections [25] and extinction of the photoelectrons as they travel through the monolayer. Spectra are acquired for monolayers as deposited, and after annealing in UHV or in air.

TABLE I
TEMPERATURE DEPENDENCE OF THE APPARENT WORK OF ADHESION AS OBTAINED FROM THE DETACHMENT LENGTHS AND EQUATION (2)

	Apparent Work of Adhesion (μJ/m^2)			
Temperature	V-FDTS	L-FDTS	V-FDDMCS	L-FDDMCS
20 °C	2.8	4.1	12.6	4.9
100 °C	2.5	4.9	7.7	3.5
200 °C	2.0	3.5	4.3	3.2
300 °C	1.4	1.4	4.1	10.2

III. RESULTS AND DISCUSSION

The effect of annealing on detachment length for the different coatings investigated is shown in Fig. 2. The detachment length plotted is a direct measure of the apparent work of adhesion of the cantilever beams (2). The apparent work of adhesion calculated from (2) is shown in Table I. The evolution of stiction with temperature showcases interesting differences between the different monolayers investigated. FDTS coated surfaces display an increase in the detachment length upon annealing, even for temperatures as high as 300 °C. This reduction in adhesion for FDTS is similar for both liquid and vapor phase deposition, but is more significant for liquid deposition. The reduction of stiction after annealing is consistent with the recommendation by Bunker *et al.* [26] to anneal FDTS covered surfaces at 150 °C to remove some loosely bound aggregates from the surface. It is worth emphasizing that both FDTS coatings have low stiction up to 300 °C and could be employed up to this temperature. The standard deviation obtained from the actuation of four different chips coated with V-FDTS (all released and coated separately) is shown in the error bars of Fig. 2.

The FDDMCS coated cantilevers have a lower detachment length than their FDTS counterparts at all temperatures investigated. In the same fashion as for FDTS surfaces, FDDMCS

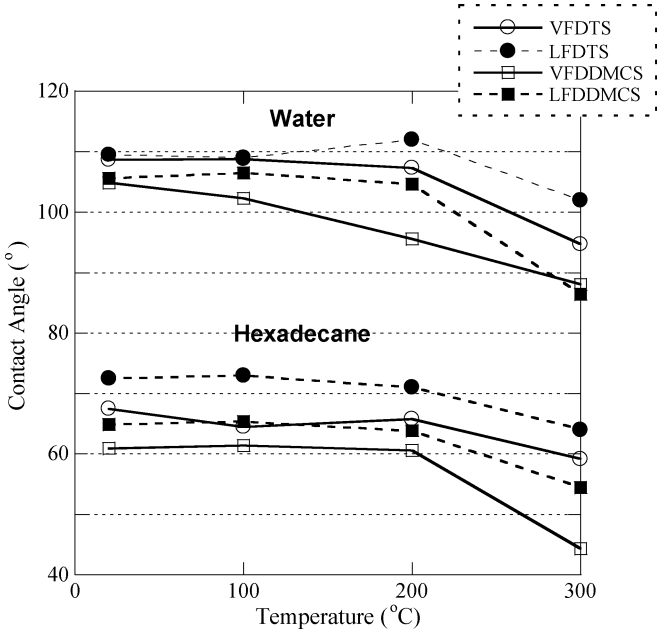

Fig. 3. Effect of annealing on water and hexadecane contact angles. The annealing time is the same as that for the measurement of the detachment length.

covered surfaces display a slight decrease in adhesion when annealed up to 200 °C. However, samples actuated at 300 °C show a large increase in stiction and the subsequent actuation at room temperature also reveals an increased stiction compared with that measured prior to the anneal at 300 °C. From the measurement of the detachment length, it can be inferred that micromachines coated with FDDMCS should not be exposed to temperatures higher than 200 °C. The data suggest that a crosslinked monolayer coating (e.g., FDTS) leads to enhanced temperature stability and allows for micromachines to maintain their function when exposed to elevated temperatures.

FDTS deposited from the liquid phase (L-FDTS) has higher stiction than FDTS deposited from the vapor phase (V-FDTS). This is probably due to the stronger tendency of liquid deposited monolayers to form sticky aggregates. The opposite behavior is observed for FDDMCS monolayers where liquid phase deposition has lower stiction than vapor phase. FDDMCS is much less likely to form aggregates due to the lack of cross-linking head group. The deposition kinetics is much slower for FDDMCS than for FDTS. The difference between L-FDDMCS and V-FDDMCS could be caused by a better coverage in the case of the L-FDDMCS (the lower coverage of the V-FDDMCS is corroborated by XPS data).

In the measurement of the detachment length at different temperatures, the same cantilever beam array is actuated more than once. Multiple actuation of the same cantilever beam array could, in principle, affect the detachment length in a similar way as temperature. To address this concern, a parallel experiment is conducted where the arrays on a single chip are actuated only once at a single annealing temperature (a different temperature for each array). In these experiments, an increase in detachment length is observed with temperature, similar to the one shown in Fig. 2. This finding is corroborated by de Boer *et al.* [8], who have also found the apparent work of adhesion to be independent of the number of actuations at relative humidity less than 90%.

The impact of annealing on the static contact angle is investigated using Si (100) test chips coated with the different monolayers studied. After each annealing step, water and hexadecane static contact angles are measured (in air at room temperature). The dependence of annealing temperature on contact angle is shown in Fig. 3. The standard deviation for each measurement is $\pm 3°$. Prior to annealing, the water contact angle for a monolayer is independent of the mode of deposition (vapor or liquid), though there is a small difference in the hexadecane contact angle, probably due to a different degree of packing or tilt of the monolayer. However, the FDTS monolayer deposited from the liquid phase (L-FDTS) systematically has a higher water and hexadecane contact angle than FDDMCS. The lower contact angles for the FDDMCS monolayers are probably caused by the steric hindrance of the two methyl groups, which produces a lower grafting density and higher tilt on the surface [27]. Also, the lower contact angle for FDDMCS can be explained by the slower deposition kinetics, which makes it more difficult to reach a high quality monolayer [28].

Upon annealing, the differences between the various monolayers are subtle, but some general trends are common to all the surfaces studied. In all cases, the contact angle of the vapor deposited monolayer is affected by annealing more than the liquid equivalent. In addition, the largest drop in contact angle occurs after annealing to 300 °C, but some small changes are already observable after 200 °C. Films deposited from the vapor phase might be of slightly lower quality than those deposited from the liquid phase, explaining why liquid phase films maintain a higher water and hexadecane contact angles upon annealing. Interestingly, a decrease in the hydrophobicity of FDTS monolayers is not accompanied by a similar decrease in antistiction properties shown in Fig. 2. This highlights the importance of directly measuring the effect of an anti-stiction monolayer with a MEMS test structure rather than relying on flat surface characterizations alone.

Tapping mode AFM measurements are performed to verify if a change in surface topography could explain the reduced adhesion upon heating. Fig. 4 displays the effect of annealing on the surface topography for the polysilicon landing pads, the polysilicon under the cantilever beams and for a Si(100) wafer covered with the monolayer. The beams are removed from the structure with double sided tape for imaging. All surfaces are covered with a FDTS monolayer deposited from liquid phase. This is chosen for imaging because it is the monolayer studied that is the most likely to display a measurable change in surface roughness (if any) caused by annealing due to its propensity to form particles during deposition [26].

As seen in Fig. 4, no significant change in surface roughness (as measured by the root-mean-square (rms) values) is observed upon annealing. The amount of particulates (and by consequence the surface roughness) is more a function of the monolayer deposition variables than a function of annealing. Indeed, a larger variation in surface roughness of the Si(100) is observed from batch to batch than upon annealing (and also at different location on the samples). Fig. 5 shows AFM images of the Si(100) test chip surfaces coated with the different monolayers before and after annealing to 300 °C. As seen, no significant effect of annealing on the rms of the surfaces is observed. It is therefore concluded that changes observed in the detachment lengths cannot be explained by a temperature-induced change in surface roughness as suggested by Ali *et al.* [6].

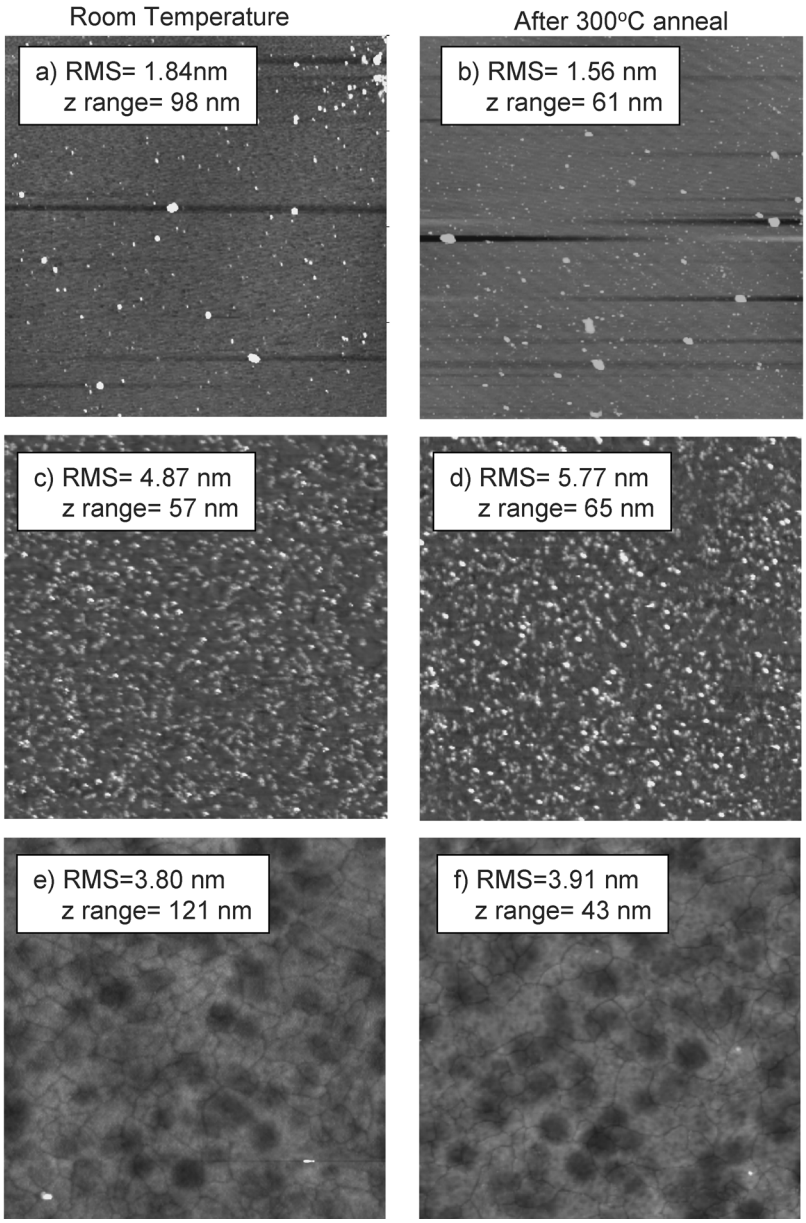

Fig. 4. Tapping mode AFM images of L-FDTS films. The left column represents the unannealed surfaces while the right column represents the annealed surfaces (up to 300 °C). (a) and (b) are 10 μm^2 images of the Si (100) test surface. (c) and (d) are 20 μm^2 images of the landing pad. (e) and (f) are 5 μm^2 images under the cantilever beams.

X-ray photoelectron spectroscopy is used to investigate the effect of annealing on the chemical nature of the monolayers. Films of FDTS and FDDMCS on Si(100) (deposited both from liquid and from vapor) are analyzed by XPS as deposited. Sequences of vacuum annealing experiments to 100, 300, 450 °C (and 500 °C for L-FDTS) are performed. The samples are cooled to room temperature after each annealing step for photoelectron spectrum acquisition. Different samples processed in the same batch as those annealed in vacuum are annealed in air following the same procedure as the one for the micromachines up to 300 °C and then analyzed by XPS. Table II summarizes the analysis of the spectra.

The main conclusions we can draw from the XPS experiments are the following. An ideal monolayer packing is achieved with FDTS deposited from liquid phase (here we take the packing of a Langmuir–Blodgett monolayer deposited just below the monolayer collapse pressure as a reference for ideal packing standard [29]). The F/Si ratio of as-deposited L-FDTS films is slightly higher than expected, probably owing to the presence of partial bilayers or particulate agglomerates. The ideal ratio is essentially recovered upon annealing to 100 °C and remains high (and roughly constant) up to 300 °C. Packing of V-FDTS films appears to be slightly inferior, and a significant decrease in the F/Si ratio is observed for annealing at 300 °C. V-FDTS films do appear to degrade faster than L-FDTS upon annealing to 450 °C. It is worth noting the similar F/Si ratios for the films annealed in air and the ones annealed in vacuum. This similarity could highlight a similar decomposition mechanism. The FDDMCS films possess much looser packing, most likely due to the steric hindrance of the two methyl sidegroups bonded to Si. Also, the

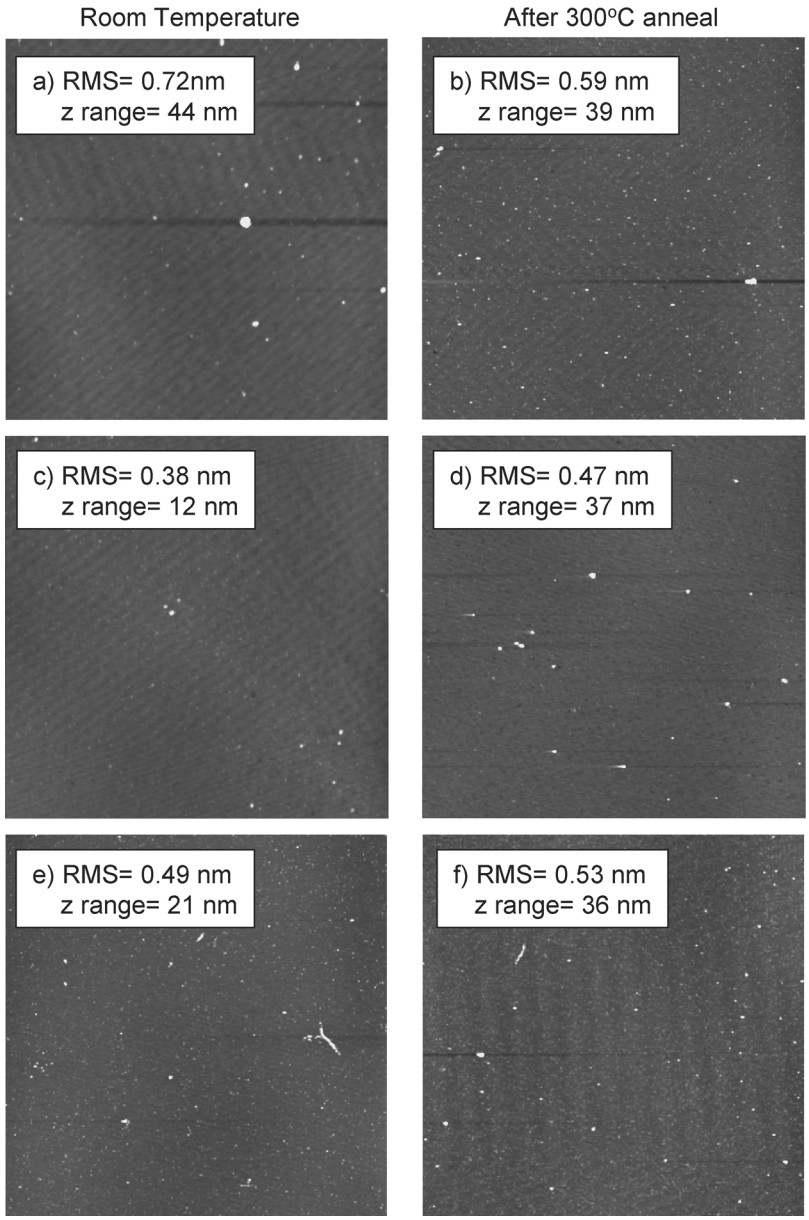

Fig. 5. Tapping mode AFM images (all from Si(100) test surfaces and for 10 $\mu\mathrm{m}^2$ areas). The left column is for the unannealed samples and the right column is for the samples after annealing at 300 °C. (a) and (b) are V-FTS, (c) and (d) are L-FDDMCS, and (e) and (f) are V-FDDMCS.

fluorine content of the films decreases more substantially upon annealing, even to the moderate temperature of 100 °C. This is undoubtedly caused by the looser packing (with consequently reduced van der Waals attraction between chains) and perhaps also by the impossibility to form a covalent siloxane network in the case of the monochlorinated precursor.

The fact that the $\mathrm{CF_3}/\mathrm{CF_2}$ ratio is essentially independent of annealing temperature in each film supports the conclusion that the loss of fluorine is accomplished by a loss of entire chains rather than single perfluoromethylene groups. This observation underscores an important difference between fluorinated and hydrogenated alkylsiloxane SAMs. The latter have been shown to decompose upon annealing by losing methylene groups, starting from the top of the alkyl chain (the $\mathrm{CH_3}$ terminal group desorbing first) [9], [13].

The gradual loss of entire molecules does not seem to have adverse effects on the surface energy of the film, as seen in Fig. 2. Presumably, the loss of an entire chain in the SAM is compensated by a tilt of the neighboring molecules, as evidenced by the decrease in the hexadecane contact angle in Fig. 3. The tilted monolayers have a surface energy comparable to the original one. Conversely, in the case of hydrogenated chains, the break-up of a chain caused by the loss of methylene groups leaves highly reactive sites in the film, which will promptly oxidize in air, leading to an increase in surface energy and consequently in work of adhesion. The cause of the reduced adhesion upon heating (see Fig. 2) should be traced likely to the removal of solvent or unreacted precursor molecules left in the monolayer or to the removal of some loosely bound aggregates.

Within the limits of XPS sensitivity, water in the film is not detected, nor is the formation of $\mathrm{C-O}$ or $\mathrm{C=O}$ bonds upon

TABLE II
SUMMARY OF XPS ANALYSIS

Sample	Treatment	F/Si	O/Si	CF_3/CF_2
LB-FDTS	Ref. 29	1.00	--	0.17
V-FDTS				
	As deposited	0.78	0.44	0.18
	Annealed in vacuum at 100 °C	0.71	0.45	0.19
	Annealed in vacuum at 300 °C	0.55	0.39	0.18
	Annealed in vacuum at 450 °C	0.42	0.40	0.22
	Annealed in air to 300 °C	0.56	0.45	0.20
L-FDTS				
	As deposited	1.19	0.54	0.33
	Annealed in vacuum at 100 °C	1.08	0.54	0.28
	Annealed in vacuum at 300 °C	0.99	0.57	0.33
	Annealed in vacuum at 450 °C	0.83	0.54	0.26
	Annealed in vacuum at 500 °C	0.61	0.53	0.18
	Annealed in air to 300 °C	0.92	0.60	0.39
V-FDDMCS				
	As deposited	0.51	0.51	0.21
	Annealed in vacuum at 100 °C	0.34	0.40	0.20
	Annealed in vacuum at 300 °C	0.28	0.35	0.24
	Annealed in vacuum at 450 °C	0.10	0.33	0.34
	Annealed in air to 300 °C	0.13	0.60	0.30
L-FDDMCS				
	As deposited	0.63	0.50	0.29
	Annealed in vacuum at 100 °C	0.57	0.51	0.23
	Annealed in vacuum at 300 °C	0.48	0.52	0.24
	Annealed in vacuum at 450 °C	0.37	0.51	0.19
	Annealed in air to 300 °C	0.32	0.56	0.22

annealing. However, while FDTS samples behave very similarly upon annealing in air or vacuum, the FDDMCS films show a substantially higher degradation when annealed in air. Presumably, the looser packing of these films affects their ability to withstand diffusion of airborne water or oxygen through the monolayer accompanied by etching of the film at or near the base of the chains.

IV. CONCLUSION

The surface adhesion of micromachines coated with two perfluorinated alkylsiloxane monolayers is characterized as a function of temperature ranging from room temperature to 300 °C. For each monolayer, two modes of deposition are investigated, namely vapor phase and liquid phase. Adhesion measurements show a consistent increase in the detachment length (reduced adhesion) for FDTS upon annealing to 300 °C. Both monolayers sustain a wide temperature range but FDTS is more stable (regardless of the deposition method), most likely due to the highly crosslinked nature of the monolayer. The increase in detachment length with temperature, which is attributed to loss of loosely bound aggregates or unreacted precursor molecules, could not have been directly predicted by contact angle measurements (showing a slight decrease in the hydrophobic nature of both monolayers with annealing) or AFM imaging (no significant change in surface roughness measured for the studied temperature range). This underscores the importance of conducting micromachine stiction measurements rather than relying solely on techniques such as AFM or contact angle measurements.

The effect of annealing in vacuum (up to 450 °C) on the chemical composition of the films is characterized by carrying out XPS measurements on Si(100). XPS analysis show that FDDMCS starts to desorb even upon annealing to 100 °C. FDTS monolayers have a better temperature stability than FDDMCS monolayers. XPS measurements highlight the mechanism for the thermal decomposition of perfluorinated alkylsiloxane monolayers, namely the monolayers lose the fluorine during annealing by loss of the entire monolayer chain. This is drastically different from alkylsiloxane monolayers, which decompose by the successive removal of methyl groups from the surface, starting with the top-most CH_3 endgroup. This mode of desorption observed for FDTS does not seem to affect stiction behavior because the chains left are able to tilt to maintain a hydrophobic surface of comparable surface energy to the pristine monolayer. Understanding the mechanism of thermal decomposition of perfluorinated alkylsiloxanes gives a direct insight in the root of the high temperature stability of those monolayers compared to alkylmonolayers such as OTS.

REFERENCES

[1] R. Maboudian, W. R. Ashurst, and C. Carraro, "Tribological challenges in micromechanical systems," *Tribol. Lett.*, vol. 12, pp. 95–100, 2002.
[2] R. Maboudian and R. T. Howe, "Critical review: adhesion in surface micromechanical structures," *J. Vacuum Sci. Technol. B*, vol. 15, pp. 1–20, 1997.
[3] R. Maboudian and C. Carraro, "Surface chemistry and tribology of MEMS," *Annu. Rev. Phys. Chem.*, vol. 55, pp. 35–54, 2004.
[4] N. Tas, T. Sonnenberg, H. Jansen, R. Legtenberg, and M. Elwenspoek, "Stiction in surface micromachining," *J. Micromech. Microeng.*, vol. 6, pp. 385–397, 1996.
[5] U. Srinivasan, M. R. Houston, R. T. Howe, and R. Maboudian, "Alkyltrichlorosilane-based self-assembled monolayer films for stiction reduction in silicon micromachines," *J. Microelectromech. Syst.*, vol. 7, pp. 252–260, 1998.
[6] S. M. Ali, J. M. Jennings, and L. M. Phinney, "Temperature dependence for in-use stiction of polycrystalline silicon MEMS cantilevers," *Sens. Actuators A—Phys.*, vol. 113, pp. 60–70, 2004.
[7] M. P. de Boer, P. J. Clews, B. K. Smith, and T. A. Michalske, "Adhesion of polysilicon microbeams in controlled humidity ambients," *Mater. res. Soc. Proc. 518*, pp. 131–136, 1998.

[8] M. P. de Boer, J. A. Knapp, T. A. Michalske, U. Srinivasan, and R. Maboudian, "Adhesion hysteresis of silane coated microcantilevers," *Acta Materialia*, vol. 48, pp. 4531–4541, 2000.
[9] G. J. Kluth, M. Sander, M. M. Sung, and R. Maboudian, "Study of the desorption mechanism of alkylsiloxane self-assembled monolayers through isotopic labeling and high resolution electron energy-loss spectroscopy experiments," *J. Vacuum Sci. Technol. A*, vol. 16, pp. 932–936, 1998.
[10] C.-H. Oh, B.-H. Kim, K. Chun, T.-D. Chung, J.-W. Byun, Y.-S. Lee, and Y.-S. Oh, "A new class of surface modification for stiction reduction," in *Transducers '99*, 1999, vol. 1, pp. 30–33.
[11] M. J. Geerken, T. S. van Zonten, R. G. H. Lammertink, Z. Borneman, W. Nijdam, C. J. M. van Rijn, and M. Wessling, "Chemical and thermal stability of alkylsilane based coatings for membrane emulsification," *Adv. Eng. Mater.*, vol. 6, pp. 749–754, 2004.
[12] M. M. Sung, G. J. Kluth, O. W. Yauw, and R. Maboudian, "Thermal behavior of alkyl monolayers on silicon surfaces," *Langmuir*, vol. 13, pp. 6164–6168, 1997.
[13] G. J. Kluth, M. M. Sung, and R. Maboudian, "Thermal behavior of alkylsiloxane self-assembled monolayers on the oxidized Si(100) surface," *Langmuir*, vol. 13, pp. 3775–3780, 1997.
[14] H. S. A. , "Lubrication of digital micromirror devices," *Tribol. Lett.*, vol. 3, pp. 247–293, 1997.
[15] B. H. Kim, T. D. Chung, C. H. Oh, and K. Chun, "A new organic modifier for anti-stiction," *Journal of Microelectromechanical Systems*, vol. 10, pp. 33–40, 2001.
[16] W. R. Ashurst, C. Carraro, and R. Maboudian, "Vapor phase anti-stiction coatings for MEMS," *IEEE Trans. Device Mater. Reliab.*, vol. 3, pp. 173–178, 2003.
[17] T. M. Mayer, M. P. de Boer, N. D. Shinn, P. J. Clews, and T. A. Michalske, "Chemical vapor deposition of fluoroalkylsilane monolayer films for adhesion control in microelectromechanical systems," *J. Vacuum Sci. Technol. B*, vol. 18, pp. 2433–2440, 2000.
[18] B. M. Dutoit, L. Barbieri, Y. von Kaenel, and P. W. Hoffmann, "Self-assembled real monlayer coating to improve release of MEMS structures," *Actuators Microsyst.*, vol. 1, pp. 810–812, 2003, Boston.
[19] D. Devaprakasam, S. Sampath, and S. K. Biswas, "Thermal stability of perfluoroalkyl silane self-assembled on a polycrystalline aluminum surface," *Langmuir*, vol. 20, pp. 1329–1334, 2004.
[20] P. W. Hoffmann, M. Stelzle, and J. F. Rabolt, "Vapor phase self-assembly of fluorinated monolayers on silicon and germanium oxide," *Langmuir*, vol. 13, pp. 1877–1880, 1997.
[21] W. R. Ashurst, "Surface Engineering for MEMS Reliability," Ph.D. dissertation, UC Berkeley, , 2003.
[22] C. H. Mastrangelo, "Adhesion-related failure mechanisms in micromechanical devices," *Tribology Letters*, vol. 3, pp. 223–238, 1997.
[23] J. F. Moulder, W. F. Stickle, P. E. Sobol, and K. D. Bomben, *Handbook of X-Ray Photoelectron Spectroscopy*. Eden Prairie, MN: Perkin-Elmer Corporation, 1992.
[24] P. Ruffieux, P. Schwaller, O. Groning, L. Schlapbach, P. Groning, Q. C. Herd, D. Funnemann, and J. Westermann, "Experimental determination of the transmission factor for the Omicron EA125 electron analyzer," *Rev. Sci. Instr.*, vol. 71, pp. 3634–3639, 2000.
[25] J. H. Scofield, "Hartree-slater subshell photoionization cross-sections at 1254 and 1487 ev," *J. Electron Spectr. Rel. Phenom.*, vol. 8, pp. 129–137, 1976.
[26] B. C. Bunker, R. W. Carpick, R. A. Assink, M. L. Thomas, M. G. Hankins, J. A. Voigt, D. Sipola, M. P. de Boer, and G. L. Gulley, "The impact of solution agglomeration on the deposition of self-assembled monolayers," *Langmuir*, vol. 16, pp. 7742–7751, 2000.
[27] J. Genzer, K. Efimenko, and D. A. Fischer, "Molecular orientation and grafting density in semifluorinated self-assembled monolayers of mono-, di-, and trichloro silanes on silica substrates," *Langmuir*, vol. 18, pp. 9307–9311, 2002.
[28] A. Y. Fadeev and T. J. McCarthy, "Trialkylsilane monolayers covalently attached to silicon surfaces: wettability studies indicating that molecular topography contributes to contact angle hysteresis," *Langmuir*, vol. 15, pp. 3759–3766, 1999.
[29] S. Ohnishi, T. Ishida, V. V. Yaminsky, and H. K. Christenson, "Characterization of fluorocarbon monolayer surfaces for direct force measurements," *Langmuir*, vol. 16, pp. 2722–2730, 2000.

Joëlle Fréchette received the B.Eng. degree from École Polytechnique de Montréal, QC, Canada. Subsequently, she received the Ph.D. degree from Princeton University, Princeton, NJ, focusing on forces at electrified interfaces using the surface forces apparatus.

She completed her postdoctoral work at the University of California, Berkeley, investigating surface adhesion for MEMS. She is currently an Assistant Professor in the Department of Chemical and Biomolecular Engineering at the Johns Hopkins University, Baltimore, MD. Her research interests are in surface forces and interfacial phenomena.

Roya Maboudian received the Ph.D. degree from the California Institute of Technology, Pasadena.

She is a Professor in the Department of Chemical Engineering and Associate Director of the Center of Integrated Nanomechanical Systems at the University of California, Berkeley. Her recent work has focused on the tribological issues in micro- and nanoelectromechanical systems and development of novel processes for materials integration for high-performance MEMS/NEMS. She and her group have designed surface processes to reduce adhesion and friction in MEMS and are currently developing methods to integrate semiconductor nanowires into Si MEMS devices.

Dr. Maboudian is the recipient of several awards, including the Presidential Early Career Award for Scientists and Engineers, the National Science Foundation Young Investigator award, and the Beckman Young Investigator award.

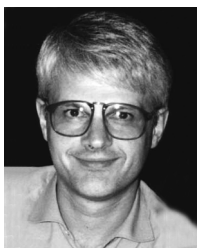

Carlo Carraro received the Bachelor's degree from the University of Padua, Padua, Italy, and the Ph.D. degree from California Institute of Technology, Pasadena.

He is a Researcher in the Department of Chemical Engineering at the University of California, Berkeley. His research interests are in the physics and chemistry of surfaces and low-dimensional structures. He has published over 80 papers in scholarly journals.